Pergamon

PII: S0968-4328(97)00034-6

Micron Vol. 28, No. 6, pp. 459–467, 1997
© 1997 Elsevier Science Ltd
All rights reserved. Printed in Great Britain
0968-4328/97 $17.00+0.00

Accurate Measurements of Crystal Structure Factors Using a FEG Electron Microscope

G. REN,* J. M. ZUO† and L.-M. PENG*

**Beijing Laboratory of Electron Microscopy, Chinese Academy of Sciences, P.O. Box 2724, Beijing 100080, P.R. China*
†*Department of Physics, Arizona State University, Tempe, AZ 85287, U.S.A.*

(*Accepted* 16 *January* 1997)

Abstract—An experimental procedure for the accurate measurement of crystal structure factors is described. This procedure is based on the use of a field emission gun electron microscope equipped with a Gatan Imaging Filter (GIF) system. The slow-scan CCD camera of the GIF system is first characterized and a constrained least squares restoration scheme is used for the deconvolution of the experimentally recorded raw elastic CBED patterns. The procedure has been applied for the accurate measurement of the (111) and (222) structure factors of silicon single crystal. A residual χ^2 value of 2.87 is achieved and the determined structure factors agree well with previous measurements using X-ray and electron diffraction techniques. © 1997 Elsevier Science Ltd. All rights reserved

Key words: structure factors, CBED, GIF, FEG, dynamical electron diffraction.

INTRODUCTION

It is now well established that the technique of convergent-beam electron diffraction (CBED) can be used quantitatively for accurate measurements of low-order crystal structure factors (Zuo *et al.*, 1988; Saunders *et al.*, 1995; Høier *et al.*, 1993). The measurements are based on quantitative comparison between experimentally measured elastic CBED pattern and computer simulations (Spence and Zuo, 1992). Experimental results are usually obtained utilizing energy filtering facilities (Spence, 1993), and simulations are carried out using Bloch wave theory of dynamical electron diffraction (Bethe, 1928).

The bonding effect is usually small. When converted to X-ray structure factors, the effect is typically of the order of 1–2% for low-order structure factors and vanishes for high-order structure factors. Extreme care must therefore be retained throughout the measurements. To ensure that theoretical results may be compared with experimentally recorded CBED pattern intensities, the illuminated area of the specimen must be free of defects and uniform in thickness. For most materials, a small probe of electron is a must for the accurate measurement of the crystal structure factors. For this reason, the use of a field emission gun electron microscope is highly advantageous here.

Most published results have been obtained either based on a serial detection technique (Zuo and Spence, 1991) or a parallel device such as a Zeiss electron microscope fitted with Omega energy filter (Deininger *et al.*, 1994). In principle, the parallel detection is in favour of the serial technique. This is because the parallel detection technique takes much less time (typically less than 2 s) in recording a two-dimensional diffraction pattern than the serial technique, the later is typically more than 100 times slower. In the case of systematic diffraction, a line scan is often used in the serial detection to reduce the recording time (Zuo and Spence, 1991). In parallel recording, however, it is necessary to have pixel by pixel resolution and uniform response. The current digital detectors of slow scan CCD camera and imaging plates all suffer from channel mixing or cross-talk effects (see below for a detailed discussion) to a varying degree. In the case of CCD camera, it is necessary to perform a gain normalization procedure to remove the gain variation from pixel to pixel, which relies on the microscope's ability to obtain a uniform illumination (Zuo, 1996). In this paper we will report a procedure which we used in the Beijing Laboratory of Electron Microscopy (BLEM) for the accurate measurement of crystal structure factors using a Gatan Imaging Filter (GIF) fitted into a field emission gun (FEG) electron microscope. In particular, we will describe a deconvolution procedure for minimizing the channel mixing effects. Our procedure has been applied for the measurement of the low-order crystal structure factors of a silicon crystal, and our results agree well with previous measurements using X-ray and electron diffraction techniques.

CHARACTERISTICS OF SSCCD

In this study we used a Philips CM200/FEG electron microscope which is equipped with a GIF system. This electron microscope has a nominal operating voltage of 200 keV and the probe size used in the present study is of the order of 14 Å. The primary beam energy of the electron microscope was calibrated by fitting a [441] higher-order Laue zone (HOLZ) pattern obtained from

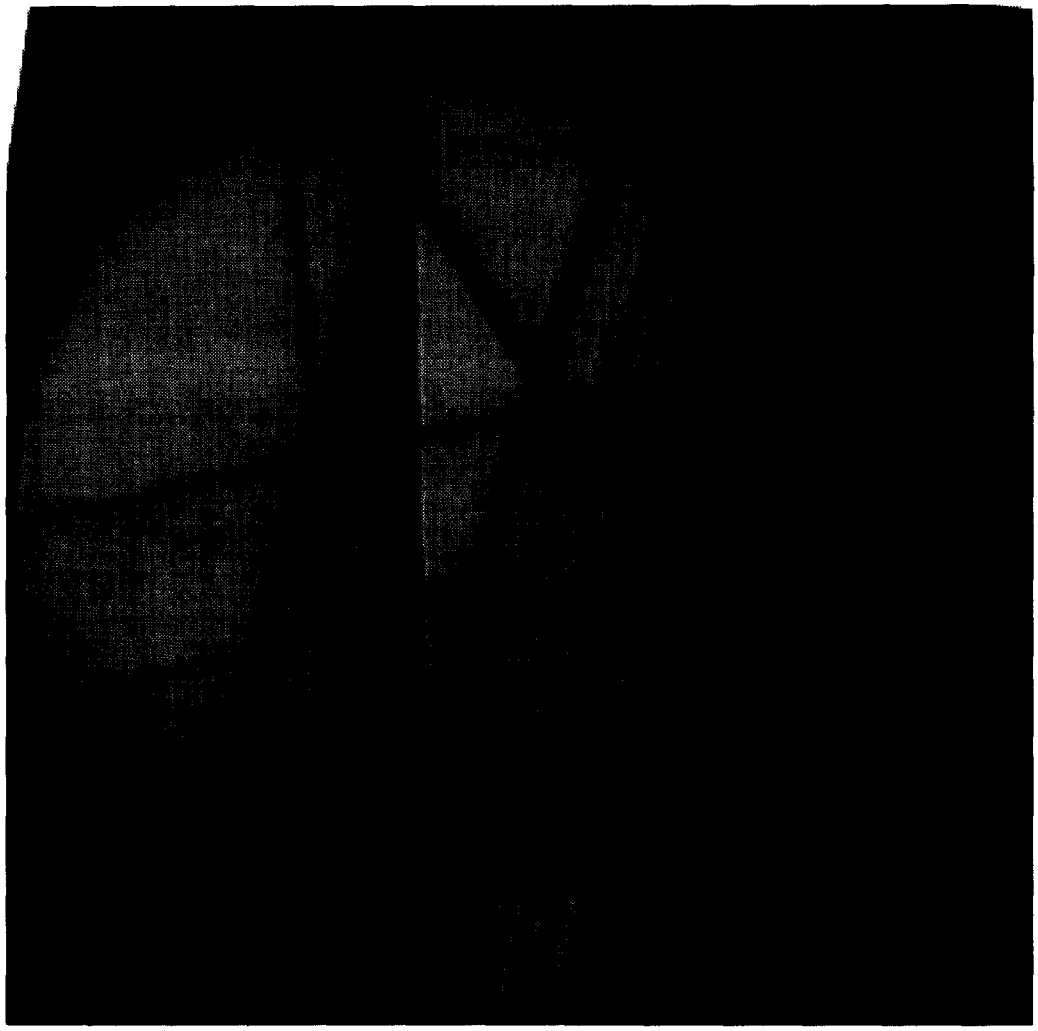

Fig. 1. (a).

a single crystal of silicon obtained using a 200 keV primary beam energy with computer simulated HOLZ patterns with varying acceleration voltage. Our best fit (Fig. 1) shows that the primary beam energy is 196.15 keV. The measured high voltage is significantly lower than the nominal value because of the GIF, which adjusts the microscope accelerating voltage for energy-filtering purpose.

Energy filtered diffracted beam intensities were obtained using a GIF system with an energy window of 10 eV, and elastic CBED patterns were recorded digitally by the slow-scan CCD (SSCCD) camera of the GIF system. The resolution and noise performance of a SSCCD is characterized by the modulation transfer function (MTF) and detector quantum efficiency (DQE), respectively. Briefly, in a SSCCD, the electron detection process may be divided into three separate stages (Ishizuka, 1993; Zuo, 1996): (1) the conversion of incident electrons into photons in the scintillator; (2) transport of the converted photons of the scintillator to the CCD array via fibre optic or lens coupling; and (3) conversion of photons to well electrons and readout of well electrons in CCD. Mathematically these processes may be expressed as follows

$$I(i,j)=\int_{y_j-\Delta y/2}^{y_j+\Delta y/2}\mathrm{d}y\int_{x_i-\Delta y/2}^{x_i+\Delta y/2}\mathrm{d}x\left[g\iint I_0(X,Y)h(X-x,Y-y)\mathrm{d}X\mathrm{d}Y\right]+B(i,j), \quad (1)$$

in which $I(i,j)$ is the readout count of the SSCCD from a pixel having index (i,j), $I_0(x,y)$ is the intensity distribution on the entrance face of the scintillator, $h(x,y)$ represents the channel mixing effects due to the spreading of electrons in the scintillator and photon propagation to the CCD array, $B(i,j)$ denotes the background signal of the CCD, and g is called the conversion coefficient or overall gain of the SSCCD camera.

The overall gain g depends on a number of factors. Effectively, this gain may be defined as the ratio between the average number of readout of the CCD $\bar{I}$ and the incident electron dose per pixel $\bar{I}_0$

$$g=\frac{\bar{I}}{\bar{I}_0}, \quad (2)$$

and this gain may be obtained by fitting the set of experimental data $\bar{I}$ for different electron dose $\bar{I}_0$ using a

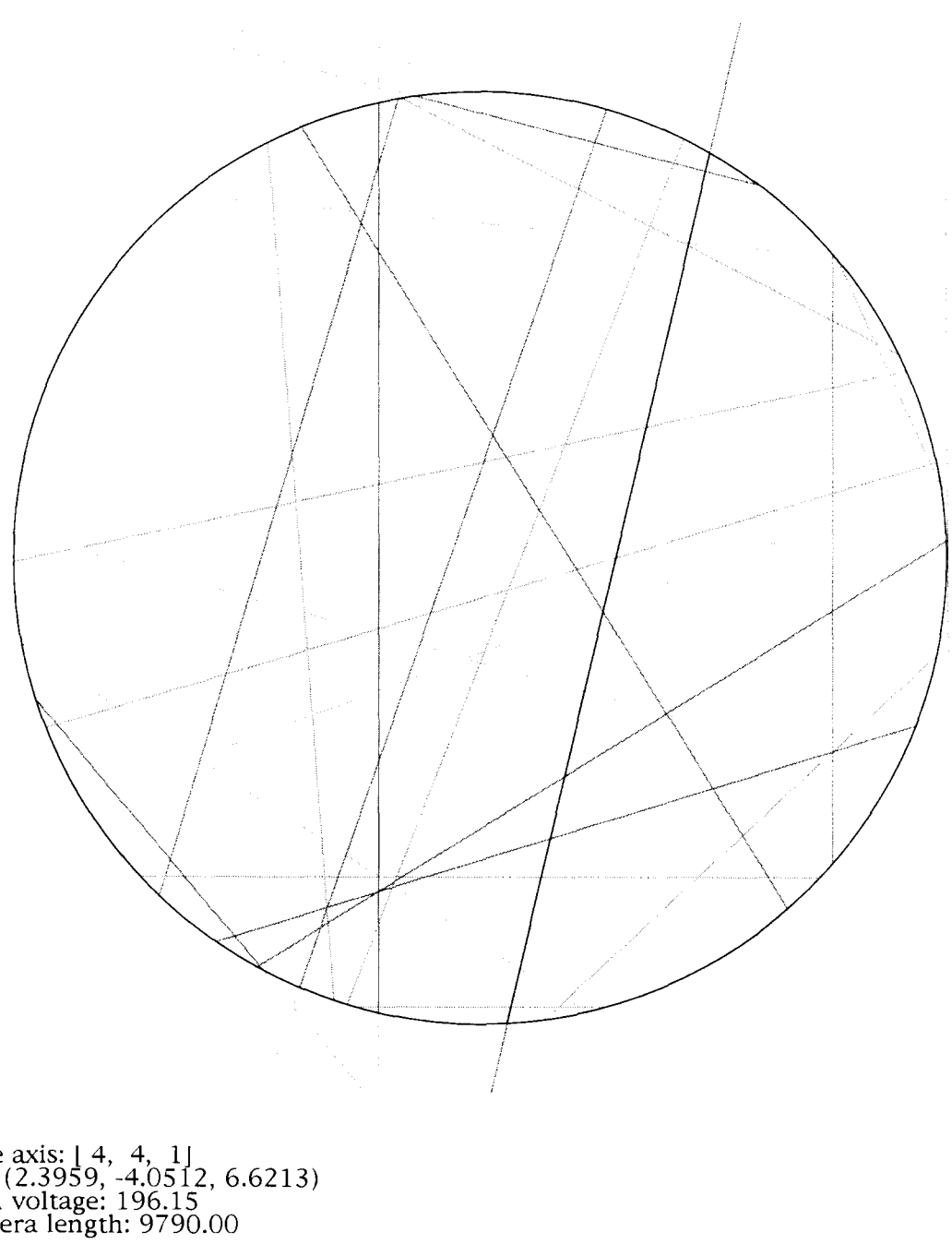

Fig. 1. *Continued*

Fig. 1. (a) Experimental [441] HOLZ pattern and (b) computer simulation for a single crystal of silicon. The experimental HOLZ pattern was obtained using a small probe of the size of 14 Å and the computer simulation was made using 196.15 keV.

straight line (Fig. 2). For our SSCCD the overall gain is determined to be 2.2. The response of a SSCCD to a point source is called the point spread function (PSF) and this function is described as $h(x,y)$. For GIF this PSF may be assumed to be rotationally symmetric and in reciprocal space this function is related to MTF $M(q)$. It can be readily shown, see for example (Zuo, 1996), that a symmetric MTF is related to the Fourier transform $H(u,v)$ of the real space PSF by the relation

$$M(q)=|H(q,0)|. \tag{3}$$

In the present study the MTF is measured by the noise method and our result is shown in Fig. 3. The MTF is seen to consist of a relatively sharp head, flat tail and a constant background. This function may therefore be conveniently modelled with the following analytical formula

$$M(q)=\frac{a}{1+aq^2}+\frac{b}{1+\beta q^2}+c. \tag{4}$$

For our SSCCD in BLEM the fitting parameters are listed in Table 1.

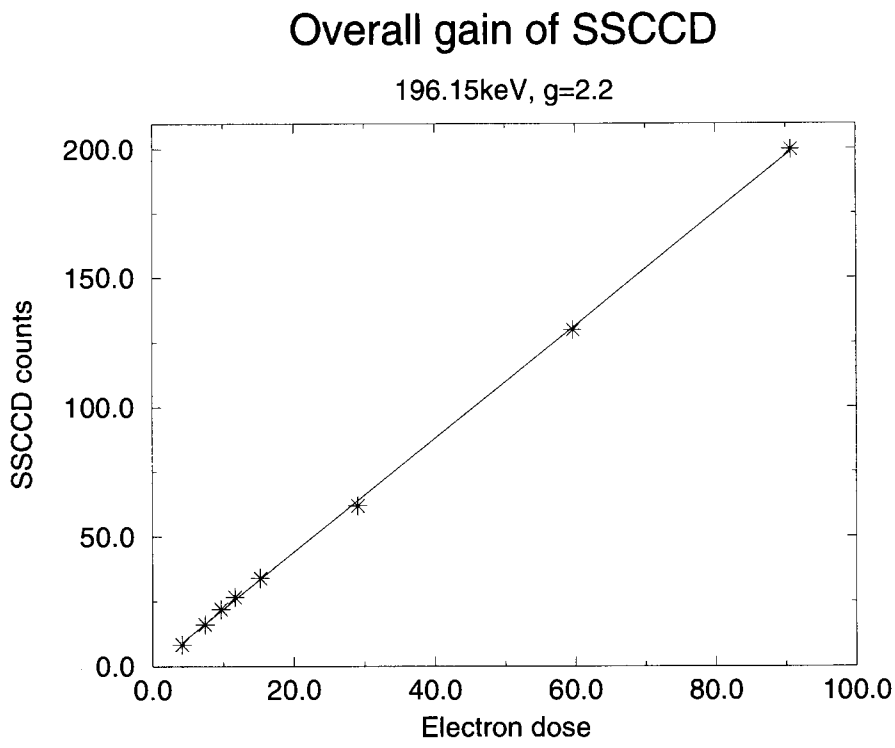

Fig. 2. Variation of the average SSCCD camera readout from a pixel as a function of the incident electron dose per pixel.

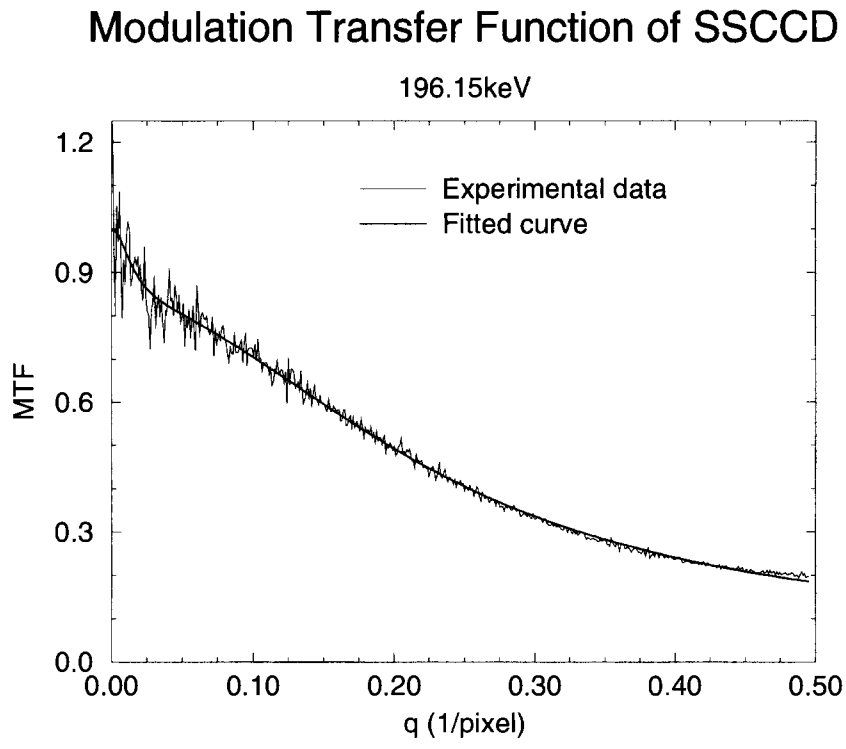

Fig. 3. Measured and fitted MTF of the Gatan SSCCD installed in the Beijing Laboratory of Electron Microscopy.

Table 1. Fitting parameters for the measured MTF curve of Fig. 3

E	a	α	b	β	c
196.15 keV	0.26243	13211	0.694	19.156	0.0436

The noise performance of a SSCCD is characterized by DQE, which is defined as the ratio between the readout signal-to-noise ratio (SNR) and the input SNR, i.e.

$$DQE=\frac{SNR^2_{\text{out}}}{SNR^2_{\text{in}}}=\frac{\bar{I}^2/\text{Var}[I]}{\bar{I}^2_0/\text{Var}[I_0]}, \tag{5}$$

in which $\bar{I}$ and $\bar{I}_0$ represent the readout and input signal, respectively, and the variances Var[I] and Var[I_0] represent that of the noise. From a set of images taken under uniform illumination with different $\bar{I}_0$, we can measure

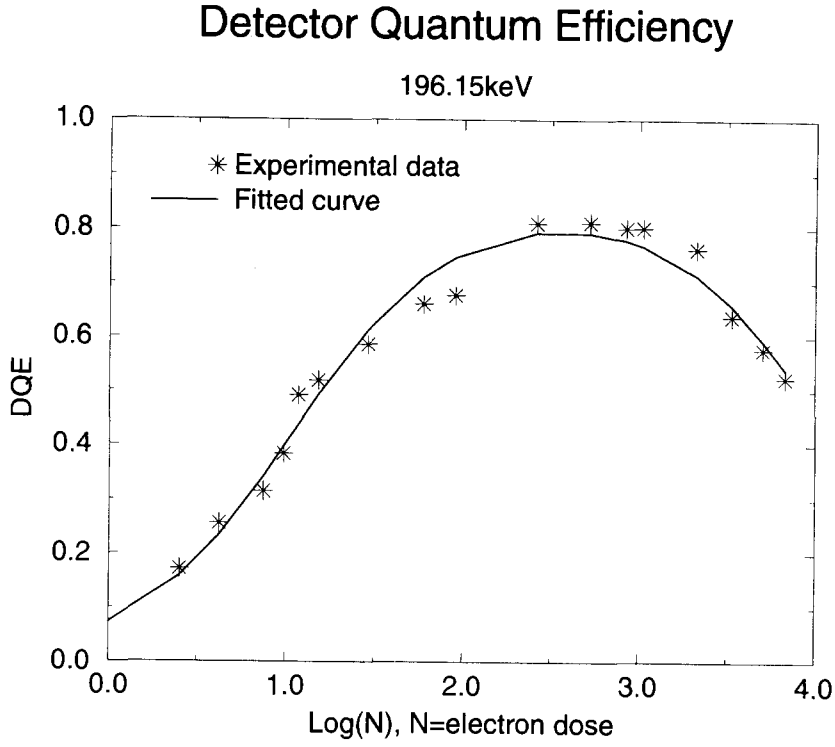

Fig. 4. Measured and fitted DQE of the Gatan SSCCD as a function of electron doses.

the read out signal $\bar{I}$ and associated noise Var[I]. It can be shown, see for example (Zuo, 1996), that

$$\mathrm{Var}[I_0]=\bar{I}_0\sum_{l,m}h^2_{l,m}, \tag{6}$$

with $h_{l,m}$ being the discrete PSF representing the contribution to a pixel with an index (i,j) from illumination at pixel (l,m). It has been shown that the dependence of the DQE on the average incident electron dose $\bar{I}_0$ is of the form

$$DQE=\left[A+B\bar{I}+\frac{C}{\bar{I}}\right], \tag{7}$$

in which A, B, C are three fitting parameters. Shown in Fig. 4 is the measured variation of the DQE with varying incident beam dose. By fitting this variation with the above analytical formula, we obtain A=1.186, B=9.83E−5 and C=12.9.

MEASUREMENT OF CRYSTAL STRUCTURE FACTORS

In general, dynamical diffracted beam intensities depend sensitively on the crystal structure factors and the crystal structure factors may be obtained from a set of diffracted beam intensities by minimizing a merit function χ^2 which measures the difference between the experimental and theoretical intensities

$$\chi^2=\frac{1}{N_{\mathrm{data}}}\sum_i\frac{(I^{\mathrm{exp}}{}_i-CI^{\mathrm{th}}{}_i-B_i)}{\sigma_i}, \tag{8}$$

in which $I^{\mathrm{exp}}{}_i$ is the experimentally measured intensity of the i-th data point, $I^{\mathrm{th}}{}_i$ is the corresponding theoretical intensity, C is a normalization constant and B_i represents the contribution from background.

Experimental raw CBED patterns were obtained using GIF fitted into a Philips CM200/FEG electron microscope. The probe size used in the present study was 14 Å and the energy window used for recording elastic CBED patterns was 10 eV. All CBED patterns were recorded using 1024 × 1024 pixels and stored in 2 byte integer format. This format provides a digital signal within the range from 0 to 65563, and each CBED pattern takes approximately 2 megabytes. To remove the channel mixing from the raw CBED pattern, we use the method of constrained least squares restoration (Gonzalez and Woods, 1992). In matrix notation and by writing the recorded two-dimensional CBED as $\mathbf{g}$, the PSF as $\mathbf{H}$ and the random noise as $\mathbf{n}$ we have

$$\mathbf{g}=\mathbf{Hf}+\mathbf{n}. \tag{9}$$

The basic idea of the restoration is to find a filter $\mathbf{Q}$ when acting on the recorded CBED pattern $\mathbf{g}$ provides an optimal estimation of the signal $\mathbf{f}$ in the sense that the recovered signal should be as smooth as possible, i.e. the criterion is to

$$\mathrm{minimize}[\nabla^2\mathbf{f}], \tag{10}$$

Fig. 5. Elastic CBED pattern taken from a single crystal of silicon using a systematic diffraction geometry. The pattern was obtained using a Philips CM200/FEG and GIF system. The probe size used for obtaining this CBED pattern was 14 Å, the energy window was 10 eV and the primary beam energy was 196.15 keV.

and at the same time to avoid the excessive noise amplification by satisfying the following constraint

$$|\mathbf{g}-\mathbf{H}\mathbf{f}|^2=|\mathbf{n}|^2. \tag{11}$$

Mathematically, the optimum filter can be obtained using the method of Lagrange multipliers, and the resultant estimation of the signal may be written in the reciprocal space as

$$F(u,v)=\frac{H^*(u,v)}{|H(u,v)|^2+\gamma|P(u,v)|^2}G(u,v), \tag{12}$$

in which $F(u,v)$ and $G(u,v)$ are the Fourier transform of the original and recorded CBED patterns, respectively, $P(u,v)$ is the Fourier transform of the derivative operator ∇^2 and γ is a parameter which is to be adjusted so that the constraint (11) is satisfied.

Shown in Fig. 5 is a CBED pattern taken under a systematic diffraction geometry. In this figure five CBED disks are recorded and they are 111, (000), (111), (222) and (333). Shown in Fig. 6 are two line profiles along the line AB from the raw CBED pattern and the deconvoluted pattern, respectively. The line profile taken from the deconvoluted CBED pattern is then used in equation (8) for defining the χ^2 function.

The variance for each of the experimental data points is estimated using DQE. Since for deconvoluted experimental data we may neglect the spreading occurring in the scintillator and fibre optics coupling within the SSCCD, we have then $\mathrm{Var}[I_0]=I_0$, that is the incident electrons satisfy the Poisson statistics. From the definition for DQE we then have

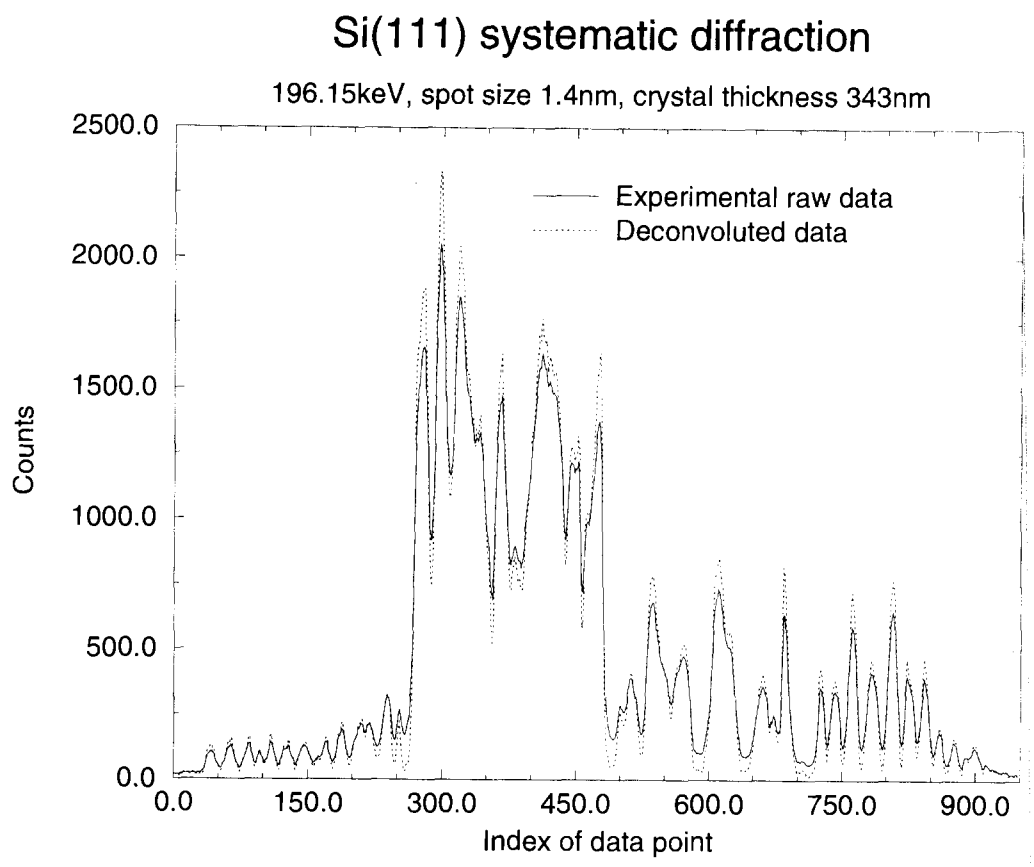

Fig. 6. Two line scans along the line AB of Fig. 5 for (a) a raw CBED pattern and (b) a deconvoluted CBED pattern.

$$\mathrm{Var}[I]=\frac{\bar{I}^2}{DQE\cdot\bar{I}_0}=\frac{g\bar{I}}{DQE}, \tag{13}$$

in which $g=\bar{I}/\bar{I}_0$ is the conversion coefficient or overall gain of the SSCCD. For our camera we have g=2.2 for 196.15 keV acceleration voltage. For any measured intensity $\bar{I}$ the associated variance $\sigma=\mathrm{Var}[I]$ is then estimated using the above formula. It should be noted that the DQE depends on the measured beam intensity $\bar{I}$, and the dependence is given by equation (5).

RESULTS

In the present study the refinement of crystal structure factors follows the procedure as described in (Zuo and Spence, 1991). This procedure utilizes a systematic diffraction geometry and our experimental CBED pattern taken for (111) systematic diffraction geometry is shown in Fig. 5. The incident beam direction was determined by comparing the experimental HOLZ pattern within the central disk with that of simulation. A line profile was extracted from the deconvoluted CBED pattern (Fig. 6) and the data was used for refinement using equation (8). In Fig. 6 the diffraction data with indices from 15 to 83 represent diffracted beam intensity variation within the 111 disk; the data with indices from 88 to 160 represent that of the transmitted beam; the data with indices from 166 to 234 represent the (111) disk and that from 238 to 306 represents the (222) disk. During the refinement only those data points within the disks were used in equation (8), and those in between disks were used to estimate the background level. It has been pointed out by Saunders (Saunders *et al.*, 1995) that in general the background level is a slow varying function of the diffraction angle. In the present study we used therefore only a uniform background level within each CBED disk.

The initial refinement was carried out by fixing all crystal structure factors to the values of neutral atom (Doyle and Turner, 1968; Bird and King, 1990; Peng *et al.*, 1996b; Peng *et al.*, 1996a) and allowing only the crystal thickness to vary. The best fit gives a residual χ^2 value of 21.15 and a crystal thickness of 3290 Å. Comparing the experimental and fitted diffraction data (Fig. 7), we can see that the fit in peak positions for the (222) disk is fairly good, while fit in other disks is reasonable, but in general the difference between the experimental and fitted curves is noticeable. The good fit in the peak positions in the (222) disk is because the fringes in this disk are mainly thickness fringes. It is seen that the peak heights are different for the two curves, indicating that the beam intensities in this disk also provide certain information on crystal structure factors (Fig. 8).

The final refinement was made for 10 fitting parameters, these are the real and imaginary parts of the [111] and [222] structure factors, the crystal thickness and the spatial coordinates of points A and B (Fig. 5). The best fit gives a residual χ^2 value of 2.87, suggesting a very good fitting. The real part of the crystal structure

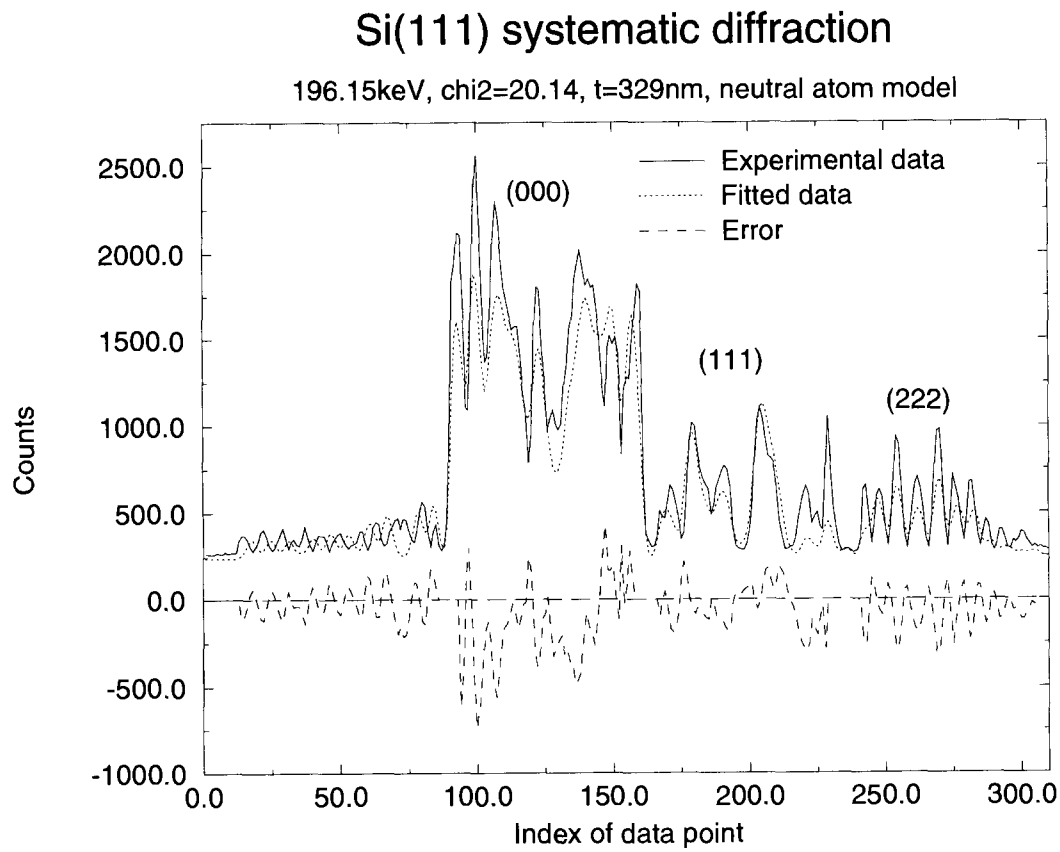

Fig. 7. Experimental and best fitted diffraction data using a neutral atom model. The residual χ^2 value returned from the fitting is 21.15, and the difference curve between the experimental and fitted data is shown below the plot.

factors determined from the fitting are $U(111)=0.47152$ $E-1\pm4.5$ $E-5$ Å^{-2} and $U(222)=0.96447$ $E-3\pm5.7$ $E-5$ Å^{-2}, and the crystal thickness is determined to be $t=3424.5\pm1.5$ Å. To compare with other measurements, the determined structure factors are converted to X-ray structure factors and the results are listed in Table 2 together with previous measurements and the estimated errors for the measurements. This table clearly shows that our results agree well with previous measurements.

The agreement between the (222) structure factors of present and the X-ray measurement by Alkire *et al.*, (Alkire *et al.*, 1982) is especially important. The Si (222) structure factor is kinematically 'forbidden' in the approximations of spherical atoms and harmonic thermal vibrations. At room temperature, the anharmonic contribution to the (222) structure factor is negligible. The measured non-zero (222) structure factor is entirely due to the non-spherical charge redistribution of chemical bonding between silicon atoms. There are a number of measurements on the Si (222) structure factors, with the measured amplitudes ranging from 0.11 to 0.2225 (see table II of Alkire *et al.*, 1982). The measurements of Alkire *et al.* (1982) use the specialized monoenergetic high energy gamma ray and relative thick crystals. Agreement of our result with this measurement shows that accurate structure factor measurement of weak reflections can be measured routinely now with the electron diffraction technique. Both the phase and amplitude of the (222) structure factor are determined by our electron diffraction measurement. The phase agrees well with the theoretical prediction. In contrast, the X-ray measurement of Alkire *et al.* (1982) is for the amplitude only.

CONCLUSIONS

In summary, in this article a procedure is described and applied to the accurate measurement of the crystal structure factors of a single crystal of Silicon. The procedure gives a set of structure factors which are within 0.2% of the measured values by X-ray crystallographers and agrees well with the recent electron diffraction measurement, and an excellent residual χ^2 value of 2.87 is achieved. Our results demonstrated that by using a FEG electron microscope and a proper deconvolution scheme, systematic errors caused by the various factors that have not been considered here in the present study, such as the specimen thickness variation and contamination, inelastic scattering and image distortion have been minimized.

Acknowledgements—This work is supported by the Chinese Academy of Sciences, the National Natural Science Foundation of China and the K. C. Wong Education Foundation, Hong Kong (JMZ), which are gratefully acknowledged.

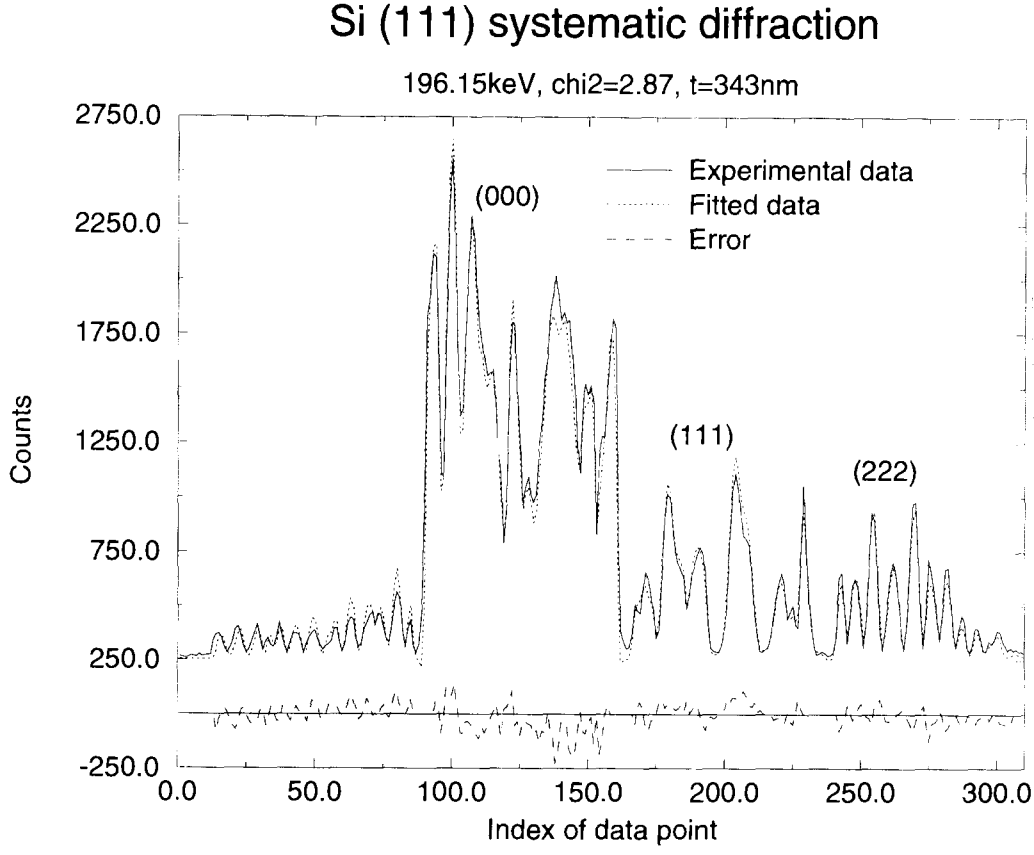

Fig. 8. Same as Fig. 7 except that the crystal structure factors are allowed to vary. The residual χ^2 value returned from the fitting is 2.87.

Table 2. Comparison between structure factors measured by different groups [electron 1 denotes present measurement and electron 2 that of Saunders *et al.* (1995)]

f_x	Neutral atom	X-ray	Electron 1	Electron 2
{111}	10.413	10.603 (3)	10.615 (5)	10.600 (9)
{222}	0.000	0.182 (1)	0.186 (4)	0.199 (7)

REFERENCES

Alkire, R. W., Yelon, W. B. and Schneider, J. R., 1982. Determination of the absolute structure factor for the forbidden (222) reflection in silicon using 0.12 Å γ rays. *Phys. Rev. B*, **26,** 3097–3104.

Bethe, H., 1928. Theorie der Beugung von Elektronen an Kristallen. *Ann. Physik.*, **87,** 55–129.

Bird, D. and King, Q., 1990. Absorptive form factor for high-energy electron diffraction. *Acta Cryst. A.*, **46,** 202–208.

Deininger, C., Necker, G. and Mayer, J., 1994. Determination of structure factors, lattice strains and accelerating voltage by energy-filtered convergent beam electron diffraction. *Ultramicroscopy*, **54,** 15–30.

Doyle, P. and Turner, P., 1968. Relativistic hartree-fock x-ray and electron scattering factors. *Acta Cryst. A*, **24,** 390–397.

Gonzalez, R. C. and Woods, R. E., 1992. *Digital Image Processing*. Addison-Wesley, Reading.

Høier, R., Bakken, L. N., Marthinsen, K. and Holmestad, R., 1993. Structure factor determination in non-centrosymmetric crystals by a two-dimensional CBED-based parameter refinement method. *Ultramicroscopy*, **49,** 159–170.

Ishizuka, K., 1993. Analysis of electron image detection efficiency of slow-scan CCD cameras. *Ultramicroscopy*, **52,** 7–20.

Peng, L.-M., Ren, G., Dudarev, S. and Whelan, M., 1996. Debye–Waller factors and absorptive scattering factors of elemental crystals. *Acta Cryst. A.*, **52.**

Peng, L.-M., Ren, G., Dudarev, S. and Whelan, M., 1996. Robust parameterization of elastic and absorptive electron atomic scattering factors. *Acta Cryst. A.* **52,** 257–276.

Saunders, M., Bird, D. M., Zaluzec, N. J., Burgess, W., Preston, A. and Humphreys, C., 1995. Measurement of low-order structure factors for silicon from zone-axis CBED patterns. *Ultramicroscopy*, **60,** 311–323.

Spence, J., 1993. On the accurate measurement of structure factor amplitude and phases by electron diffraction. *Acta. Cryst. A.* **49,** 231–260.

Spence, J. and Zuo, J., 1992. *Electron Microdiffraction*. Plenum Press, New York.

Zuo, J., 1996. Electron detection characteristics of slow-scan CCD camera. *Ultramicroscopy*, **66,** 21–33.

Zuo, J. and Spence, J., 1991. Automated structure factor refinement from convergent-beam patterns. *Ultramicroscopy*, **35,** 185–196.

Zuo, J. M., Spence, J. C. H. and O'Keeffe, M., 1988. Bonding in GaAs. *Phys. Rev. Letts.* **613,** 353–356.